Pergamon

www.neuroscience-ibro.com

PII: S0306-4522(02)00063-5

Neuroscience Vol. 112, No. 1, pp. 51–63, 2002

0306-4522/02 $22.00+0.00

NECABS: A FAMILY OF NEURONAL Ca^{2+}-BINDING PROTEINS WITH AN UNUSUAL DOMAIN STRUCTURE AND A RESTRICTED EXPRESSION PATTERN

S. SUGITA,[1] A. HO and T. C. SÜDHOF*

Center for Basic Neuroscience, Department of Molecular Genetics, and Howard Hughes Medical Institute, The University of Texas Southwestern Medical Center at Dallas, Dallas, TX 75235, USA

Abstract—Ca^{2+}-signalling plays a major role in regulating all aspects of neuronal function. Different types of neurons exhibit characteristic differences in the responses to Ca^{2+}-signals. Correlating with differences in Ca^{2+}-response are expression patterns of Ca^{2+}-binding proteins that often serve as markers for various types of neurons. For example, in the cerebral cortex the EF-hand Ca^{2+}-binding proteins parvalbumin and calbindin are primarily expressed in inhibitory interneurons where they influence Ca^{2+}-dependent responses. We have now identified a new family of proteins called NECABs (neuronal Ca^{2+}-binding proteins). NECABs contain an N-terminal EF-hand domain that binds Ca^{2+}, but different from many other neuronal EF-hand Ca^{2+}-binding proteins, only a single EF-hand domain is present. At the C-terminus, NECABs include a DUF176 motif, a bacterial domain of unknown function that was previously not observed in eukaryotes. In rat at least three closely related NECAB genes are expressed either primarily in brain (NECABs 1 and 2) or in brain and muscle (NECAB 3). Immunocytochemistry revealed that NECAB 1 is restricted to subsets of neurons. In cerebral cortex, NECAB 1 is highly and uniformly expressed only in layer 4 pyramidal neurons, whereas in hippocampus only inhibitory interneurons and CA2 pyramidal cells contain NECAB 1. In these neurons, NECAB 1 fills the entire cytoplasm similar to other EF-hand Ca^{2+}-binding proteins, and is not concentrated in any particular subcellular compartment.

We suggest that NECABs represent a novel family of regulatory Ca^{2+}-binding proteins with an unusual domain structure and a limited expression in a subclass of neurons.

Key words: interneuron, EF-hand, calcium binding protein, APP, synaptotagmin.

Ca^{2+} functions as a master regulator of neurons. Not only synaptic transmission but also membrane excitability, gene transcription, and many other processes are controlled by Ca^{2+} as an intracellular signal. Complementing the omnipotence of Ca^{2+} as a neuronal regulator are a slew of Ca^{2+}-binding proteins. Most neuronal Ca^{2+}-binding proteins (NECABs) can be classified into two groups based on the type of domain used to bind Ca^{2+}: EF-hand domain proteins such as calmodulin which are usually cytosolic and have relatively high Ca^{2+}-affinities, and C_2-domain proteins such as synaptotagmins which are generally membrane bound and have overall lower Ca^{2+}-affinities (reviewed in Baimbridge et al., 1992; Braunewell and Gundelfinger, 1999; Donato, 2001; Rizo and Südhof, 1998).

The EF-hand represents a relatively simple Ca^{2+}-binding domain in which a contiguous sequence forms a helix–loop–helix motif that coordinates a single Ca^{2+}-ion (Baimbridge et al., 1992; Lewit-Bentley and Rety, 2000). A large number of EF-hand Ca^{2+}-binding proteins is known, most of which contain at least two EF-hands that bind Ca^{2+} cooperatively. Some EF-hand Ca^{2+}-binding proteins are universally distributed in all cells, such as calmodulin, whereas others are present only in a limited number of cell types, such as troponin C. Although calmodulin is ubiquitous, it is nevertheless highly enriched in brain in neurons, whereas glia cells in brain contain high levels of another class of EF-hand Ca^{2+}-binding proteins called S100 proteins (Donato, 2001). Furthermore, several NECABs containing 2–4 EF-hands have been described that are enriched in subsets of neurons, for example calbindin and parvalbumin that are concentrated in inhibitory interneurons in the hippocampus and cerebral cortex (reviewed in Baimbridge et al., 1992; Hof et al., 1999).

The functions of EF-hand Ca^{2+}-binding proteins are diverse. The vast majority of these proteins are small proteins that are basically composed only of EF-hands, and function either as Ca^{2+}-dependent activators of tar-

[1] Present address: Division of Cellular and Molecular Biology, Toronto Western Research Institute, Canada.

*Corresponding author. Tel.: +1-214-6481876; fax: +1-214-6481879.

E-mail address: thomas.sudhof@utsouthwestern.edu (T. C. Südhof).

Abbreviations: EGTA, ethylene glycol-bis(2-aminoethyl-ether)-*N*,*N*,*N*′,*N*′-tetraacetic acid; GST, glutathione *S*-transferase; HEPES, *N*-(2-hydroxyethyl)piperazine-*N*′-(2-ethanesulfonic acid); HRP, horseradish peroxidase; NECAB, neuronal Ca^{2+}-binding protein; SDS–PAGE, sodium dodecyl sulfate–polyacrylamide gel electrophoresis; VCP, vasolin-containing peptide.

get proteins (the most well-known example again being calmodulin), or as Ca^{2+}-buffers (e.g. parvalbumin; Caillard et al., 2000; Vecellio et al., 2000). In addition, EF-hand domains in some proteins are fused to other functional domains which are regulated by the adjacent EF-hands, as best described for the Ca^{2+}-dependent protease calpain (Sorimachi and Suzuki, 2001).

In contrast to EF-hands, C_2-domains are more complex Ca^{2+}-binding domains in which multiple Ca^{2+}-binding sites are formed by discontinuous sequences in a β-sandwich structure (Rizo and Südhof, 1998; Ubach et al., 1998). The best characterized C_2-domain protein is synaptotagmin 1 (Syt 1), a synaptic vesicle protein that binds multiple Ca^{2+} ions via two C_2-domains (reviewed in Südhof and Rizo, 1996), and is required for Ca^{2+}-triggering of exocytosis but not for fusion as such (Geppert et al., 1994). The effector mechanism by which Ca^{2+} triggers synaptotagmin function has remained elusive. In a previous study (Sugita and Südhof, 2000), we had isolated a protein of approximately 40 kDa using affinity chromatography on the immobilized C_2A-domain of Syt 1. Binding of this protein to the C_2A-domain was regulated by Ca^{2+} at physiological concentrations, and was more tight than binding of any other protein. In cloning and characterizing this 40-kDa protein, we now find that it belongs to a unique family of NECABs with an unusual domain structure. Although our further studies showed that NECABs are unlikely to interact with Syt 1 physiologically, the distribution of NECAB 1 identifies it as a useful marker for a subset of neurons which may be endowed by NECAB 1 with specific properties.

EXPERIMENTAL PROCEDURES

All experiments were carried out in accordance with the animal use guidelines issued by the University of Texas, Southwestern Medical Center Institutional Animal Use Review Board and by the US Government.

Affinity chromatography on immobilized glutathione S-transferase (GST)-fusion proteins

Four frozen rat brains (Pelfreeze) were homogenized in 22 ml of 10 mM HEPES–NaOH pH 7.4, 1 mM EGTA, 0.1 g/l phenylmethylsulfonyl fluoride, 10 mg/l leupeptin, 10 mg/l aprotinin, 1 mg/l pepstatin A. An equal volume of the same buffer containing 0.2 M NaCl and 2% NP-40 was added, the homogenate was extracted for 1 h at 4°C, insoluble material was removed by centrifugation (30 min at $100\,000\times g$), and $MgCl_2$ and $CaCl_2$ were added to the supernatant to final concentrations of 2.5 and 2.0 mM, respectively. The total rat brain extract was then precleared by incubation for 2 h at 4°C with 250 µl of glutathione agarose (Sigma, St. Louis, MO, USA) followed by centrifugation ($800\times g$ for 2 min). Aliquots of the precleared brain extract (40 ml) were incubated overnight at 4°C with 0.5 ml glutathione agarose containing ~2 mg GST–Syt 1 C_2A fusion protein pre-equilibrated with buffer A (10 mM HEPES–NaOH, pH 7.4, 0.1 M NaCl, 1% NP-40, 2.5 mM $MgCl_2$, 1 mM $CaCl_2$). The various GST–C_2A domain fusion proteins used in the current experiments were described previously (Li et al., 1995; Shao et al., 1997; Südhof and Rizo, 1996; Sugita and Südhof, 2000). After the overnight incubation, the agarose was packed into polypropylene columns with a paper disc (Quick-Sep, Isolab), washed with 20 ml of buffer A, and eluted with 2 ml each of buffer A containing 0.2 and 0.5 M NaCl. Finally, the column was eluted with 2 ml of buffer A containing 5 mM EGTA instead of 1 mM $CaCl_2$. Eluates were concentrated with trichloroacetic acid from 2 ml to 120 µl, and the concentrated eluates were analyzed by sodium dodecyl sulfate–polyacrylamide gel electrophoresis (SDS–PAGE) and Coomassie Brilliant Blue staining (20 µl). Peptide sequences of the 40-kDa major binding component were obtained as described (Sugita and Südhof, 2000).

cDNA cloning of NECABs, sequencing, construction of expression vectors

BLAST searches with the six peptide sequences from NECAB 1 identified one human EST clone 1629731 (accession number AA984296) that contained three of the peptide sequences. In addition, another human EST clone 970990 (accession number AA776143) was identified that overlapped with the 5′-end of clone 1629731. Clone 970990 was purchased from Research Genetics (Huntsville, AL, USA) and fully sequenced, confirming that it encodes partial sequences of human NECAB 1. Furthermore, a BLAST search with human NECAB 1 identified two isoforms of NECAB 1 that we named them NECAB 2 (e.g. clone 24712, accession number AF070637) and NECAB 3 (e.g. clone 366285, accession number AA025666). The 0.75-kb *Bam*HI–*Eco*RV fragment from clone 970990 and the 0.8-kb *Hin*dIII fragment from clone 24712 were used to isolate cDNA clones for NECAB 1 and NECAB 2, respectively, from a rat brain cDNA library using standard procedures (Perin et al., 1990; Sambrook et al., 1989). Five independent NECAB 1 clones (pBS-NECAB 1-3, 1-4, 1-5, 1-12, 1-21) and six independent NECAB 2 clones (pBS-NECAB 2-3, 2-6, 2-17, 2-19, 2-21, 2-22) were isolated. pBS-NECAB 1-12 and pBS-NECAB 2-6 encoded full-length cDNAs for rat NECAB 1 and NECAB 2, respectively. The full-length sequence of NECAB 3 was assembled from two overlapping EST clones (IMAGE numbers 366285 and 1324936). All cDNA clones, including EST clones, were fully sequenced; the resulting sequences were submitted to GenBank (accession numbers AF193755–AF193759). Mammalian expression vectors encoding full-length NECABs were constructed as follows: pCMV-NECAB 1-1 was obtained by cloning the 1.4-kb *Nar*I–*Xba*I fragment from pBS-NECAB 1-12 into the *Cla*I–*Xba*I site of pCMV5. pCMV-NECAB 2 was obtained by inserting a 1.5-kb *Eco*RI fragment from pBS-NECAB 2-6 into the *Eco*RI site of pCMV5. pCMV-hNECAB 3 was generated by subcloning an 0.25-kb *Eco*RI fragment from IMAGE clone number 1324936 and a 1.1-kb *Eco*RI–*Hin*dIII fragment from IMAGE clone number 366285 into the *Eco*RI–*Hin*dIII sites of pCMV5. COS-7 cell transfections with pCMV vectors were performed as described (Sugita et al., 1998). The NECAB GST-fusion protein vectors were constructed as follows: pGex-NECAB 1-2 was made by cloning the 0.45-kb *Bgl*II–*Nco*I polymerase chain reaction (PCR) and the 1.3-kb *Nco*I–*Sal*I fragments from pBS-NECAB 1-4 into the *Bam*HI–*Sal*I site of pGex-KG (Guan and Dixon, 1991). pGex-NECAB 2 was generated by inserting a 1.4-kb PCR fragment with the full-length coding region into the *Nco*I–*Hin*dIII sites of pGex-KG. pGex-hNECAB 3 was obtained by subcloning an 0.20 kb *Nco*I–*Eco*RI fragment from IMAGE clone number 1324936 with the 1.1-kb *Eco*RI–*Hin*dIII fragment from pCMV-hNECAB 3 into the *Nco*I–*Hin*dIII sites of pGex-KG.

$^{45}Ca^{2+}$ overlay experiments

$^{45}Ca^{2+}$ overlay experiments were performed essentially as described (Maruyama et al., 1984; Nguyen and Südhof, 1997). Purified GST and GST-NECAB 1-2 (~10 µg) were separated by SDS–PAGE gels and transferred to nitrocellulose membranes. The membranes were incubated twice for 10 min at room temperature in 60 mM KCl, 5 mM $MgCl_2$, 10 mM imidazole–HCl (pH 6.8) with or without 10 mM $CaCl_2$. The buffer was then exchanged with fresh buffer containing 1 mCi/ml $^{45}Ca^{2+}$ (Amersham, Arlington Heights, IL, USA) and incubated for 10 min at room temperature. Membranes were washed twice

for 5 min with distilled water, dried at room temperature, and exposed to film for 40 h.

Antibodies

The polyclonal antibody for NECAB 1 (T2948) was raised against GST fusion proteins encoding NECAB 1 (GST-NECAB 1-2), and affinity purified with GST-NECAB 1-2 covalently attached to a chromatography matrix.

Immunocytochemistry

Anesthetized mice were perfusion-fixed with 4% freshly prepared paraformaldehyde, and cryostat sections were prepared and stained using either single labeling with affinity-purified NECAB 1 polyclonal antibodies followed by horseradish peroxidase (HRP)-coupled secondary antibodies, or double labeling with polyclonal NECAB 1 and monoclonal calbindin or parvalbumin antibodies (obtained from Sigma) followed by fluorescein isothiocyanate- and rhodamine-coupled secondary antibodies. Labeled sections were viewed by standard light microscopy.

Miscellaneous procedures

RNA blotting experiments were carried out as described (Sugita et al., 1998) using commercially available human multi-tissue RNA blots (Clontech, Palo Alto, CA, USA). SDS–PAGE and immunoblotting analyses were performed as described (Laemmli, 1970; Towbin et al., 1979).

RESULTS

Purification and cloning of NECABs

In order to identify potential ligands for Syt 1 that may mediate its function in Ca^{2+}-triggering of exocytosis, we used the immobilized C_2A-domain of Syt 1 as a matrix for Ca^{2+}-dependent affinity chromatography of rat brain proteins (Sugita and Südhof, 2000). Multiple proteins were purified on this column as described previously, most notably vasolin-containing peptide (VCP, Fig. 1). However, we detected only one major protein whose Ca^{2+}-dependent binding to the C_2A-domain was stable in 0.5 M NaCl. This protein was eluted from the C_2A-domain by EGTA, and was named here NECAB 1 for reasons described below. NECAB 1 bound to the immobilized C_2A-domain of Syt 1 unusually tightly as shown by two criteria. First, NECAB 1 was retained on the immobilized C_2A-domain even in the presence of 0.5 M NaCl which interferes with all other known interactions of the C_2A-domain including phospholipid binding (Zhang et al., 1998). Second, NECAB 1 was depleted from the flow-through of the Syt 1 C_2A-domain column (data not shown), suggesting a quantitative interaction.

To characterize NECAB 1, we subjected the purified protein to peptide sequencing. GenBank searches did not detect the peptide sequences in a previously reported protein. However, multiple EST clones were found that contain these or similar sequences, and encode either NECAB 1 or two closely related proteins (subsequently referred to as NECABs 2 and 3). The various EST clones were purchased, sequenced, and used to screen rat brain cDNA libraries (Sambrook et al., 1989). In this manner

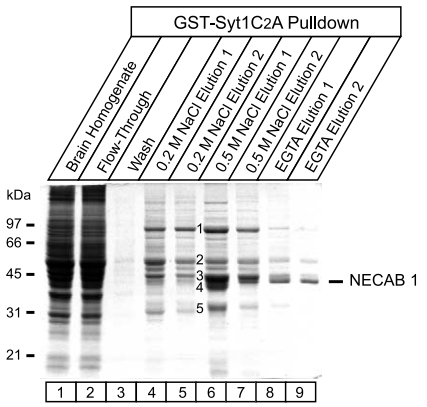

Fig. 1. Identification of NECAB 1. Rat brain proteins were subject to affinity chromatography on the immobilized C_2A-domain from Syt 1 expressed as a GST-fusion protein (GST–Syt1C_2A). Rat brain homogenate (lane 1) was passed over the GST-fusion protein column; after collection of the flow-through (lane 2) the column was washed extensively (lane 3) and eluted with increasing concentrations of NaCl in Ca^{2+}-containing buffers (lanes 4–7) followed by EGTA (lanes 8 and 9). Eluates were analyzed by SDS–PAGE and Coomassie Brilliant Blue staining. Note that after the 0.5 M NaCl elution (lane 7), the major remaining protein bound to the column and eluted with EGTA (lanes 8 and 9) is a 40-kDa protein which we named NECAB 1. Previous studies (Sugita and Südhof, 2000) identified the other proteins eluted at high salt in lanes 6 and 7 as follows: 1 = VCP; 2 = tubulin; 3 = actin; 4 = PHAP2; 5 = PHAP1 and p32. Immunoblot analysis showed that NECAB 1 is depleted in the flowthrough, suggesting high-affinity binding (not shown).

we obtained full-length and partial sequences for rat and human NECABs 1, 2 and 3.

As shown in alignment of the NECAB amino acid sequences in Fig. 2, NECABs are hydrophilic proteins of 352–362 residues that contain no recognizable transmembrane region or signal sequence. The three NECABs are homologous to each other over their entire sequence. The pattern of homology between the three NECABs is patchy, with blocks of identical residues alternating with divergent sequences. The highest degree of similarity is observed in the N-terminal region of NECABs which includes a string of 12 residues that are identical in all three NECABs (residues 39–50 of NECAB 1). The most divergence is observed in a central 45-residue stretch which displays little significant sequence homology (residues 172–216 of NECAB 1). Wherever available, the rat and human sequences of a NECAB are virtually identical, indicating a high degree of evolutionary conservation (Fig. 2). Furthermore, databank searches demonstrated that closely related sequences are expressed in many other vertebrates. However, no invertebrate NECABs were detected; in particular, no NECABs were found in the *Drosophila* and *Caenorhabditis elegans* genome sequences (data not shown).

Tissue distribution of NECAB expression

We employed RNA blotting experiments to elucidate which tissues express NECAB mRNAs (Fig. 3). NECAB 1 and NECAB 2 mRNAs were detectably synthesized only in brain. NECAB 3 was present at similar levels in brain, heart and skeletal muscle; lower signals were

```
rNECAB 1            MEDSRETSPSSNNSSEELSSALQLSKGMSIFLDILRRADKNDDGKLSFEEFKAYFADGVLSGEE   64
rNECAB 2            MGEPRAPLVPDIPAADPDPGPAAPRGGTAVILDIFRRADKNDDGKLSLEEFQLFFADGVLNEKE   64
hNECAB 3  MACAGLLTVCLLRPPAPQPQPQTPRHPQLAPDPGPAGHTLFQDVFRRADKNDDGKLSFEEFQNYFADGVLSLGE   74

rNECAB 1  LHELFHTIDTHNTNNLDTEELCEYFSQHLGEYENVLAALEDLNLSILKAMGKTKKDYQEASNLEQFVTRFLLKE  134
hNECAB 1  ..........................................................ENVLAALEDLNLSILKAMGKTKKDYQEASNLEQFVTRFLLKE   42
rNECAB 2  LEGLFHTIDSDNTNHVDTKELCDYFVEHMGDYEDVLASLETLNHSVLKAMGYTKKVYEGGNNVDQFVTRFLLKE  138
hNECAB 2  ..........................................................EDVLASLETLNHSVLKAMGYTKKVYEGGSNVDQFVTRFLLKE   42
hNECAB 3  LQELFSGIDGHLTDNLETEKLCDYFSEHLGVYRPVLAALESLNRAVLAAMDATKLEYERASKVDQFVTRFLLRE  148

rNECAB 1  TLNQLQSLQNSLECAMETTEEQTRQERQGPSKPEVLS----IQWPGKRSSRRVQRHNSFSPNSPQFNVSSPALL  208
hNECAB 1  TLNQLQSLQNSLECAMETTEEQTRQERQGPAKPEVLS----IQWPGKRSSRRVQRHNSFSPNSPQFNVSGPGLL  102
rNECAB 2  TANQIQSLLSSVESAVEAIEEQTSQIRQDYCKP---SHGVNESRYGGPTPPYIPNHKLVVPEPVK-SLPVAIGE  208
hNECAB 2  TANQIQSLLSSVESAVEAIEEQTSQLRQNHIKP---SHSAAQTWCGSPTPASAPNHKLMAMEQGK-TLPSATED  102
hNECAB 3  TVSQLQALQSSLEGASDTLEAQAHGWRSDAESVEAQSRLCGSRRAGRRALRSVSRSSTWSPGSSDTGRSS     218

rNECAB 1  EEDNQWMTQINRLQKLIDRLEKKDLKLEPLEEEVIEENTKPHIMLVQRQMSVTEEDLEEFQLALKHYVESASAQ  282
hNECAB 1  EEDNQWMTQINRLQKLIDRLEKKDLKLEPPEEEIIEGNTKSHIMLVQRQMSVIEEDLEEFQLALKHYVESASSQ  186
rNECAB 2  PKEEGLEVQISRLAELIGRLESKTLSFDLQQRLSDEEGTNMYLQLVRQEMAVCPEQLGEFLDSLRQYLRSTAEE  282
hNECAB 2  AKEEGLEAQISRLAELIGRLESKALWFDLQQRLSDEDGTNMHLQLVRQEMAVCPEQLSEFLDSLRQYLRGTTGV  186
hNECAB 3  EAEMQWRLQVNRLQELIDQLECKAPRLEPLREEDLAKGPDLHILMAQRQVQVAEEGLQDFHRALRCYVDFTGAQ  292

rNECAB 1  SGCLRISIQKLSNESRYMIYEFWENSSVWNRHLQTNYSKTFQRSNVDFLETPELTSTMLVPASWWILKNN*    352
hNECAB 1  SGCLRISIQKLSNESRYMIYEFWENSSVWNSHLQTNYSKTFQRSNVDFLETPELTSTMLVPASWWIL-NN*    255
rNECAB 2  KNCFHVAAVRMADGLTFVIYEFWETEEEWKKHLQSPVCKGFRHVKVDTLSQPEALSQISVPAAWCTSGRD*    352
hNECAB 2  RNCFHITAVRLSDGFTFVIYEFWETEEAWKRHLQSPLCKAFRHVKVDTLSQPEALSRILVPAAWCTVGRD*    256
hNECAB 3  SHCLHVSAQKMLDGASFTLYEFWQDEASWRRHQQSPGSKAFQRILIDHLRAPDTLTIVFFPASWWIMNNN*    362
```

Fig. 2. Amino acid sequences of NECABs 1, 2 and 3. The amino acid sequences for rat and human NECABs as deduced from cDNA sequences are aligned for maximal homology. Residues shared among the majority of sequences are highlighted. NECAB 1 peptide sequences determined from the protein purified by Syt 1 affinity chromatography (Fig. 1) are underlined. Sequences are identified on the left (r = rat; h = human) and numbered on the right. Note that the human NECAB 1 and 2 sequences are partial at the N-terminus.

also detected in pancreas. Two mRNAs were detected for NECAB 3 in muscle, but not in brain. Both muscle mRNAs are large enough to encode full-length NECAB 3. The expression data suggest that NECABs are primarily synthesized in brain, with NECAB 3 also expressed in other excitable tissues.

Characterization of NECAB 1 protein

To analyze the properties of NECAB 1, especially its potential interaction with Syt 1, we raised antibodies to recombinant NECAB 1. We then examined the specificity of the antibodies using COS cells transfected with control DNA (salmon sperm DNA) or with NECAB 1, 2 and 3 expression vectors. Comparison of the immunoblotting signal obtained with NECAB 1 antibodies in transfected COS cells and brain homogenates shows that the antibody strongly recognized NECAB 1 (Fig. 4). The size of the protein corresponded to the single band obtained in brain homogenates. Fig. 4 also demonstrates that the antibody cross-reacts with NECABs 2 and 3 which migrate at slightly smaller apparent molecular weight than NECAB 1. No band corresponding to NECABs 2 and 3 were detected in brain

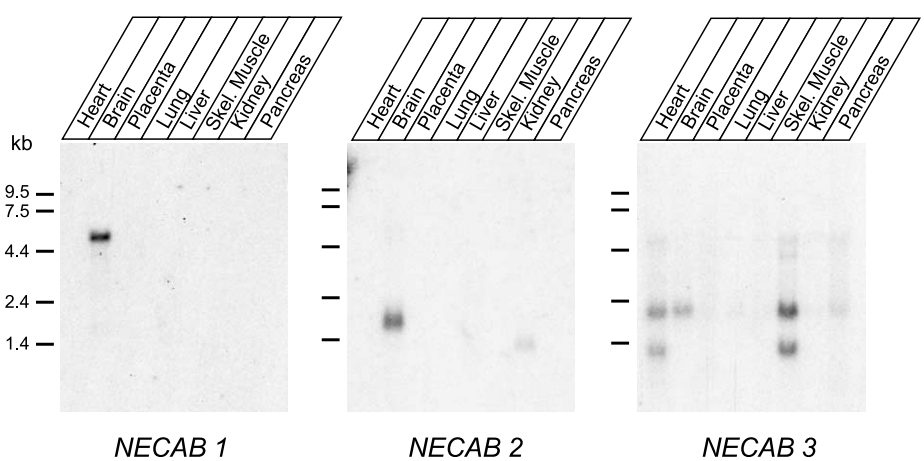

Fig. 3. RNA analysis of the tissue distribution of expression for NECABs 1, 2 and 3. Western blots containing poly(A)+-enriched RNAs from the indicated human tissues were hybridized with probes specific for NECAB 1, 2 and 3 as marked. Numbers on the left indicate the positions of molecular weight markers.

homogenates (Fig. 4). This result indicates that the relative affinity of the antibody for NECABs 2 and 3, and/or the abundance of NECABs 2 and 3 in brain are too low for the antibody to react with NECABs 2 and 3 in brain. Thus, at the level of sensitivity of immunoblotting, the antibody is specific for NECAB 1 in brain.

We next investigated the tissue distribution of NECAB 1 by immunoblotting to confirm the RNA blotting results, and examined the levels of NECAB 1 during brain development. NECAB 1 protein was only detected in brain and no other tissue tested (upper panel in Fig. 5). VCP, by contrast, was found to be similarly expressed in most tissues investigated (lower panel in Fig. 5). In vertebrates, the majority of synapses in brain are assembled postnatally after the overall structure and composition of the brain has been established. As a result, many brain-specific proteins are expressed relatively early during development, except for synaptic proteins whose abundance increases dramatically postnatally (Daly and Ziff, 1997). When we analyzed the abundance of NECAB 1 in brain homogenates as a function of development, we observed a similar postnatal increase in the abundance of this protein (Fig. 6). Although NECAB 1 and Syt 1 were both detectable at birth, their levels were low compared to those of ubiquitous VCP (P1 in Fig. 6), but exhibited a large increase over the next weeks. This result suggests that NECAB 1 may function in mature neurons connected by synapses.

Ca^{2+}-dependent protein–protein interactions of NECAB 1

The C_2A-domain of Syt 1 is an interesting Ca^{2+}-binding domain which binds a cluster of three Ca^{2+}-ions via two sequence loops on top of the domain (Ubach et al., 1998), and interacts with phospholipids and with syntaxin 1 and VCP as a function of Ca^{2+} (Davletov and Südhof, 1993; Kee and Scheller, 1996; Li et al., 1995; Sugita and Südhof, 2000). Because we isolated NECAB 1 as a Ca^{2+}-dependent interactor of Syt 1, we first studied its binding to the C_2A-domain of Syt 1 in detail. Purification of NECAB 1 on the immobilized C_2A-domain requires Ca^{2+}, suggesting that NECAB 1 binds to the top Ca^{2+}-binding loops of the C_2A-domain as previously described for syntaxin 1 (Fig. 1) (Shao et al., 1997). This hypothesis was confirmed in binding experiments with a mutant C_2A-domain of Syt 1 (D230N) in which a single residue of the Ca^{2+}-binding site was mutated (data not shown). With this mutant C_2A-domain, no NECAB 1 binding could be obtained, indicating that Ca^{2+}-binding to the C_2A-domain is essential for the interaction.

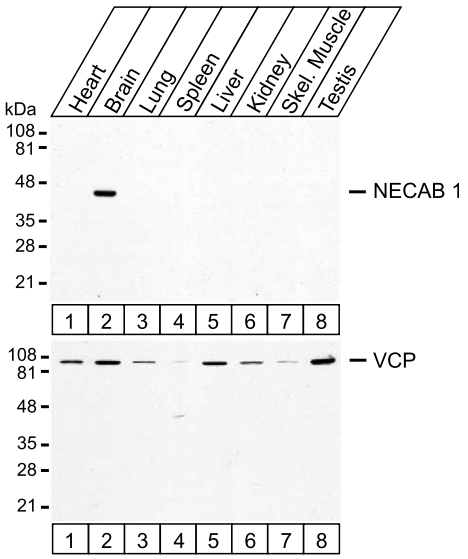

Fig. 5. Tissue distribution of NECAB 1 expression analyzed by immunoblotting. Homogenates of the indicated rat tissues (50 µg protein/lane) were subjected to SDS–PAGE and immunoblotting with antibodies to NECAB 1 (top panel) and VCP (bottom panel; used as a ubiquitously expressed protein control). Numbers on the left indicate positions of molecular mass markers.

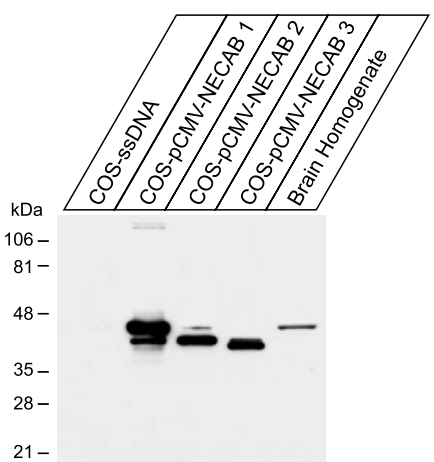

Fig. 4. Characterization of NECAB antibodies. COS-7 cells were transfected with salmon sperm DNA (COS-ssDNA) or with NECAB 1, 2 and 3 expression vectors (COS-pCMV-NECAB 1, -NECAB 2, and -NECAB 3). Proteins from transfected COS cells and from rat brain homogenate were analyzed by SDS–PAGE and immunoblotting with affinity-purified polyclonal antibodies against NECAB 1. Numbers on the left indicate positions of molecular weight markers. Note that although the antibody weakly crossreacts with all three NECABs, it preferentially recognizes NECAB 1 in brain.

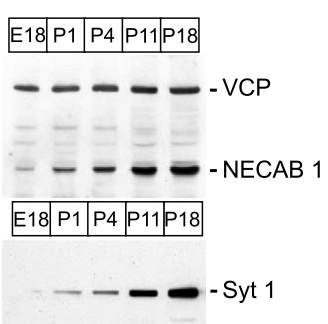

Fig. 6. Developmental profile of NECAB 1 protein expression. Brain homogenates (30 µg) from rats of the indicated ages (embryonic day (E) 19; postnatal days (P) 1, P4, P11, P18) were analyzed by immunoblotting with antibodies against VCP, NECAB 1, and Syt 1 as indicated.

The intrinsic Ca^{2+}-affinity of the Syt 1 C_2A-domain is low; full occupancy of all three Ca^{2+}-binding sites is achieved only at Ca^{2+}-concentrations approaching 1 mM (Zhang et al., 1998). As a result, Ca^{2+}-dependent interactions of the C_2A-domain with syntaxin 1 or VCP also exhibit a low Ca^{2+}-affinity (Li et al., 1995). Interestingly, however, phospholipid-binding to the C_2A-domain occurs at low micromolar Ca^{2+}-concentrations even though occupancy of all three Ca^{2+}-binding sites is required (Zhang et al., 1998). This suggests that normally the coordination sites for the three Ca^{2+}-ions are incompletely occupied in the C_2A-domain, and that phospholipids provide additional coordination sites, thereby increasing the apparent Ca^{2+}-affinity of the C_2A-domain. To test if NECAB 1 behaved like syntaxin 1 and VCP in the Ca^{2+}-dependent interactions with the C_2A-domain, we examined the Ca^{2+}-dependence of its binding to the C_2A-domain. To our surprise, we observed that NECAB 1 binding was observed even at nominally zero Ca^{2+}-levels (Fig. 7A). Presumably the nominally Ca^{2+}-free buffer contains contaminating endogenous Ca^{2+} at micromolar concentrations, thereby leading to NECAB 1 binding which could be completely reversed by Ca^{2+}-chelation with EGTA (Fig. 2). NECAB 1 binding to the C_2A-domain of Syt 1 was maximal at low micromolar concentrations of Ca^{2+} while VCP, as described previously for syntaxin 1 (Li et al., 1995), required millimolar Ca^{2+}-concentrations. However, when we reversed the binding experiment and used GST-NECABs as an affinity matrix, we obtained no binding of Syt 1 (Fig. 7B).

During the course of this study a paper reported a partial sequence for NECAB 3 (named XB51) as a potential interactor for another protein we had previously cloned and called Mint 2 which was renamed X11L2 in that study (Lee et al., 2000). In order to test this interaction, we immunoblotted the proteins that bound to NECABs in the presence or absence of Ca^{2+} with antibodies to Mint 2 (Fig. 7B). No binding of Mint 2 to NECABs was detected, arguing against a strong interaction. Finally, to execute an unbiased search for NECAB interactors, we searched for binding proteins that bind only to immobilized NECAB 1. A single specific protein was identified on Coomassie-stained SDS gels (data not shown). Sequencing identified this protein as *N*-copine, a neuron-specific protein that contains two C_2-domains like Syt 1 but differs from Syt 1 in that it is a soluble protein that is not enriched on synaptic vesicles (Nakayama et al., 1998).

Domain structure of NECAB 1 includes a functional EF-hand, Ca^{2+}-binding site and a prokaryotic C-terminal domain

To gain insight into potential functions of NECABs, we analyzed their sequences using the conserved domain databank of NCBI. Two domains were identified: the highly conserved N-terminal sequence of NECABs contains an EF-hand domain, and the C-terminal sequence contains a DUF176 motif (Fig. 8). In addition, the N-terminal sequence following the short EF-hand

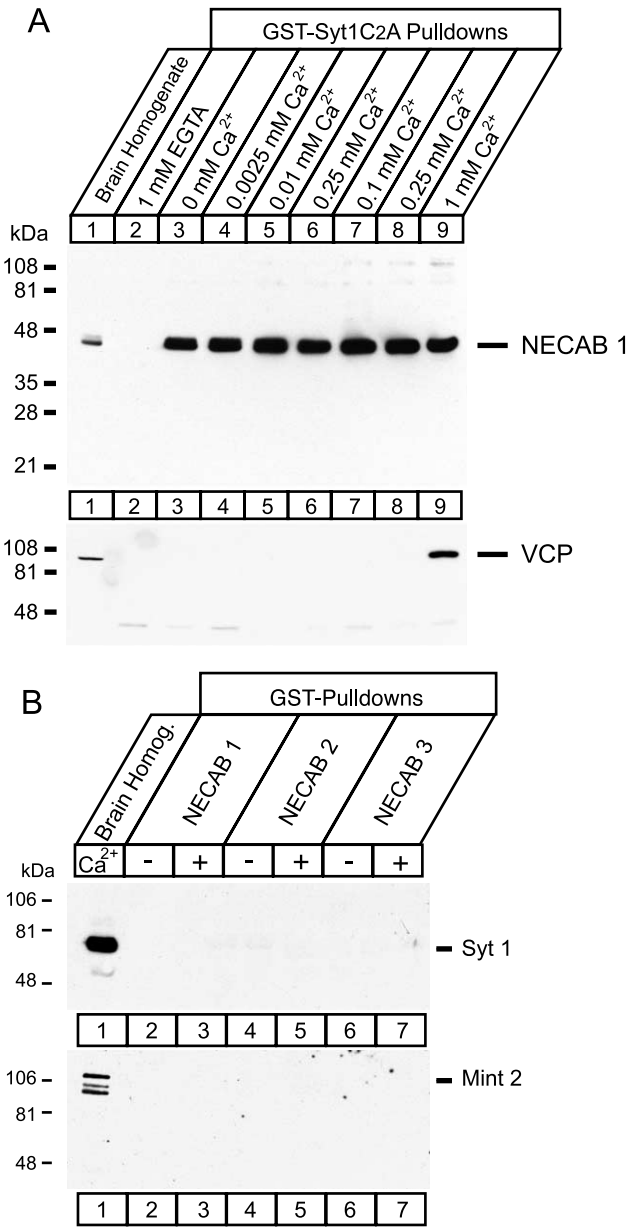

Fig. 7. Protein–protein interactions of NECAB 1. (A) Ca^{2+}-dependence of NECAB 1 binding to the Syt 1 C_2A-domain fusion protein. Rat brain proteins were bound to immobilized GST-fusion protein containing the C_2A-domain of Syt 1 in the presence of the indicated Ca^{2+} concentrations and 2.5 mM Mg^{2+}. Bound proteins were eluted with 5 mM EGTA and analyzed by immunoblotting for NECAB 1 (top) and VCP (bottom). Molecular mass markers are indicated on the left. Note that both NECAB 1 and VCP are highly enriched from the homogenate by binding to the C_2A-domain (compare lanes 1 and 9) but that NECAB 1 even binds at nominally 0.0 mM calcium, presumably because of contaminating low µM concentrations of calcium (lane 3). (B) Lack of binding of Syt 1 and Mint 2 to GST-NECAB fusion proteins. Rat brain proteins were subjected to affinity chromatography on immobilized GST-fusion proteins containing NECABs 1, 2 and 3 in the absence and presence of Ca^{2+} as indicated. Bound proteins were analyzed by immunoblotting for Syt 1 and Mint 2. In both panels, numbers on the left indicate positions of molecular weight markers.

domain is highly conserved among all NECABs, although not homologous to other proteins in the current databases (Fig. 2), and we therefore refer to this sequence as the NECAB homology region (NHR).

Alignment of the N-terminal NECAB sequences with those of EF-hand proteins reveals a strong degree of conservation in which all of the typical Ca^{2+}-binding residues are retained (Fig. 8B) (Kawasaki et al., 1998; Nelson and Chazin, 1998). To test if NECAB 1 actually binds Ca^{2+}, we used $^{45}Ca^{2+}$-blotting as a measure of Ca^{2+}-binding (Maruyama et al., 1984) which we have previously applied to GST-fusion proteins (Nguyen and Südhof, 1997). Purified GST-NECAB 1 fusion protein or GST alone were blotted onto nitrocellulose membranes and incubated with $^{45}Ca^{2+}$ in the presence or absence of cold Ca^{2+}. Bound $^{45}Ca^{2+}$ was visualized by autoradiography, revealing specific binding by NECAB 1 (Fig. 9). These data confirm that NECAB 1, and probably other NECABs as well, contains a functional Ca^{2+}-binding site.

The presence of a DUF176 domain in NECABs is surprising. Although no function is known for the DUF176 domain, its presence is nevertheless interesting because this domain was up to now only identified in bacterial proteins (Wasinger and Humphery-Smith, 1998). Most proteins containing the DUF176 domains are very small proteins of unknown function. Alignment of the NECAB sequences with the DUF176 sequences from bacteria (Fig. 8C) unequivocally demonstrates that this domain is present in NECABs. Appearance of this domain in a NECAB that is specific to vertebrates is unexpected, and suggests either that the domain was evolutionarily introduced into eukaryotes very late, possibly by lateral gene transfer, or lost in evolutionarily older animals.

Immunolocalization of NECAB 1 in brain

We employed affinity-purified NECAB 1 antibodies to examine the expression of NECAB 1 in brain. Fig. 10 shows that NECAB 1 displays a distinctive expression pattern as observed in coronal sections of mouse brain. NECAB 1 appears to be exclusively neuronal, and restricted to a subset of brain areas. In general, white matter is unlabeled. Moreover, most cortical structures also lack NECAB 1, and NECAB 1 is more abundant in rostral than in caudal brain regions (Fig. 10). For example, in cerebral cortex only layer 4 is strongly stained, and the cerebellum lacks significant levels of NECAB 1. Some thalamic nuclei contain high levels of NECAB 1 (e.g. the mediodorsal nucleus), whereas others (e.g. the lateral nucleus) do not (Fig. 10).

To examine the localization of NECAB 1 at higher magnification, we studied the hippocampus and cortex (Fig. 11). The distribution of NECAB 1 as revealed by immunocytochemistry in the hippocampus was highly unusual: no granule cell neurons in the dentate gyrus or pyramidal neurons in the CA regions were labeled except for a small band of pyramidal neurons at the boundary between CA1 and CA3 (Fig. 11A). However, dense labeling of interneurons in the hilus was observed (Fig. 11B, C), as were strongly labeled interneurons interspersed throughout the hippocampus proper (Fig. 11D). High magnification views demonstrated that not only the cell bodies of the neurons but also their dendritic projections were labeled, consistent with a soluble cytosolic protein. In the cortex, the strongest labeling was detected in layer 4 but scattered NECAB 1-positive neurons were found throughout the depth of the cortex, with particular enrichment in layer 2 (Fig. 11E). As observed for the hippocampus, cortical neurons were filled entirely with NECAB 1, and dendrites were also strongly labeled (Fig. 11F–H).

The staining pattern for NECAB 1 in hippocampus is reminiscent of that observed for small Ca^{2+}-binding proteins such as calbindin and parvalbumin (Gulyas et al., 1999). To investigate if NECAB 1 colocalizes with calbindin or parvalbumin, we analyzed hippocampal sections by double immunofluorescence labeling (Fig. 12). All calbindin-positive neurons also contained NECAB 1, although many more neurons contain only NECAB 1, but not calbindin (Fig. 12A–C). In contrast, most parvalbumin-positive neurons lack NECAB 1 (Fig. 12D–F), suggesting that NECAB 1 is not present in all interneurons.

DISCUSSION

In the present study, we have followed up on recent results which identified a single protein that bound to the C_2A-domain of Syt 1 with high affinity at physiological Ca^{2+}-concentrations (Sugita and Südhof, 2000). In studying this protein, we have now molecularly characterized a new family of neuronal Ca^{2+}-binding proteins that we named NECABs. NECABs are hydrophilic proteins that contain three regions of homology: a short N-terminal EF-hand domain that appears to be a functional Ca^{2+}-binding motif based on $^{45}Ca^{2+}$-binding experiments (Fig. 9), a 'pioneer' N-terminal sequence that is highly conserved among NECAB isoforms but does not display significant similarity to other proteins, and a C-terminal DUF176 domain that was previously only observed in bacteria (Figs. 2 and 8). NECABs are primarily expressed in brain, although NECAB 3 is also present in other excitable tissues (heart and skeletal muscle). In brain, NECAB 1 is highly concentrated in a subset of neurons with a distribution that differs from that of other Ca^{2+}-binding proteins (Figs. 10–12). For example, in cerebral cortex a high density of NECAB 1-positive neurons is only observed in layer 4 pyramidal cells, whereas in hippocampus inhibitory interneurons in the hilus appear to be most strongly labeled. The expression of NECAB 3 in brain, heart, and skeletal muscle is striking because it suggests a function for NECAB 3 in excitable tissues. However, NECAB 3 protein was not studied in the current paper, and it is unknown if the protein is truly synthesized in all of these tissues.

NECABs were discovered because of the tight and stoichiometric binding of NECAB 1 to the C_2A-domain of Syt 1. However, when we attempted to reproduce this interaction with independent assays (e.g. GST-NECAB

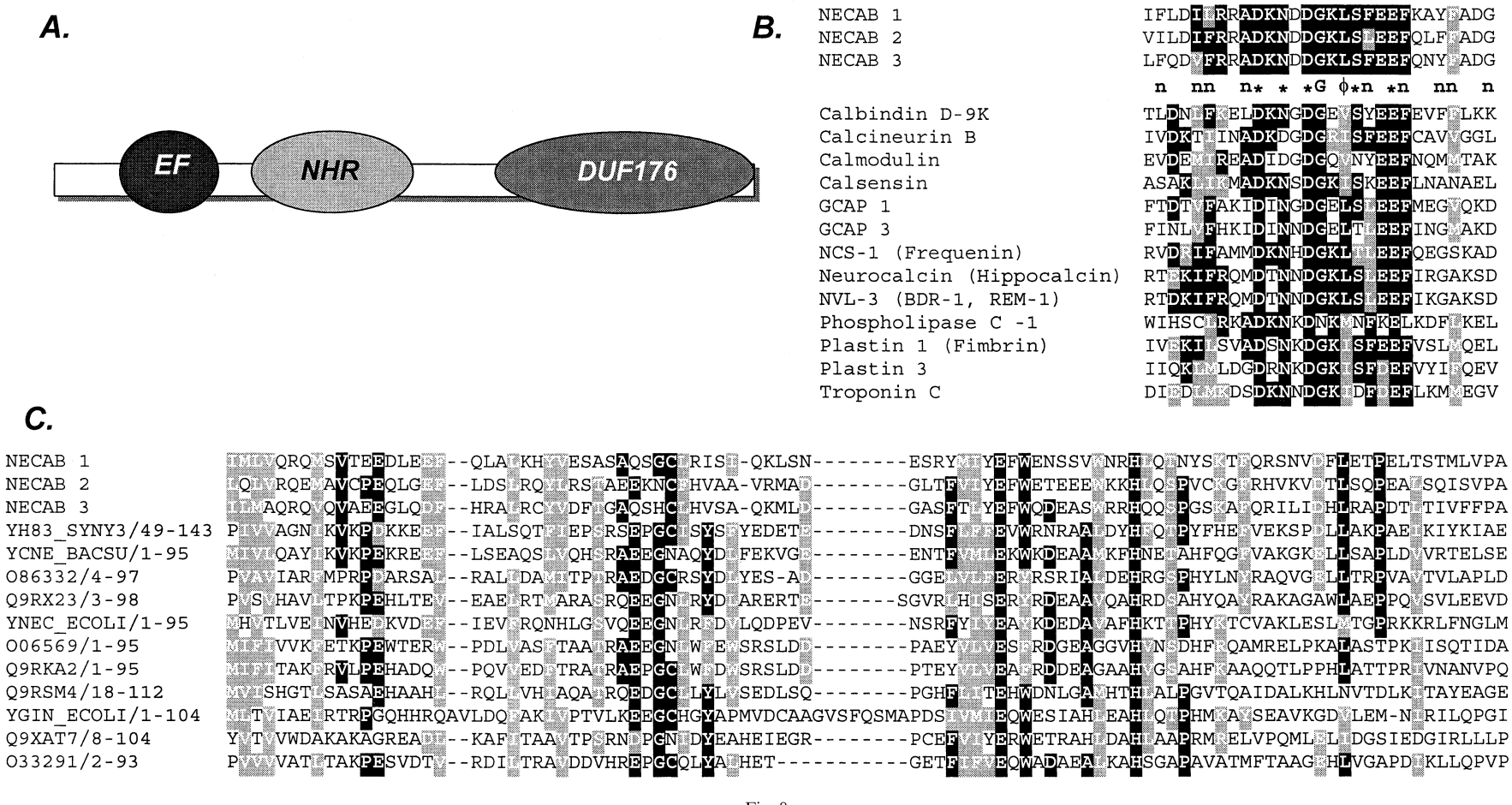
A.
EF
NHR
DUF176
B.
NECAB 1
NECAB 2
NECAB 3
n nn n* * *G ϕ*n *n nn n
Calbindin D-9K
Calcineurin B
Calmodulin
Calsensin
GCAP 1
GCAP 3
NCS-1 (Frequenin)
Neurocalcin (Hippocalcin)
NVL-3 (BDR-1, REM-1)
Phospholipase C -1
Plastin 1 (Fimbrin)
Plastin 3
Troponin C
C.
NECAB 1
NECAB 2
NECAB 3
YH83_SYNY3/49-143
YCNE_BACSU/1-95
O86332/4-97
Q9RX23/3-98
YNEC_ECOLI/1-95
O06569/1-95
Q9RKA2/1-95
Q9RSM4/18-112
YGIN_ECOLI/1-104
Q9XAT7/8-104
O33291/2-93

Fig. 8

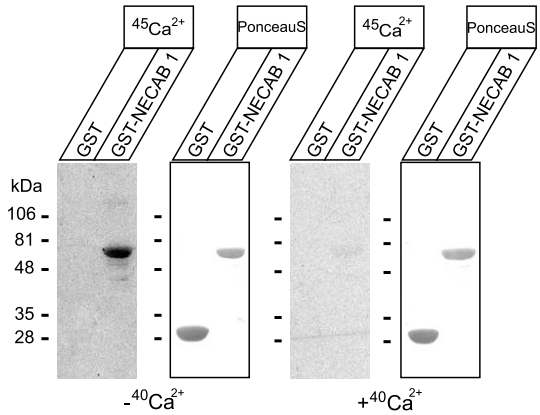

Fig. 9. Ca^{2+}-binding to NECAB 1 analyzed by $^{45}Ca^{2+}$ blotting. GST and a GST-NECAB 1 fusion protein were separated by SDS–PAGE and analyzed by blotting with $^{45}Ca^{2+}$ in the absence or presence of 10 mM cold $^{40}Ca^{2+}$. The same blots were stained by Ponceau S to visualize protein on the blot. Numbers on the left indicate positions of molecular weight markers.

affinity chromatography or immunoprecipitations), we failed to confirm the interaction (Fig. 7B). Thus, in spite of the fact that NECAB 1 is the only currently known binding protein for the C_2A-domain of Syt 1 that binds stoichiometrically at physiological Ca^{2+}-concentrations, it is questionable if this *in vitro* interaction reflects a physiological interaction. Similarly, during the course of this study a partial NECAB 3 sequence was reported as that of a protein binding to Mint 2 (named as X11L2 in that study; Lee et al., 2000). Again, we were unable to reproduce any binding. Since the original study also reported only limited evidence for an interaction, it seems likely that NECABs do not physiologically bind Mint 2. The doubts about a physiological relevance of these interactions is reinforced by the finding that the only protein found to specifically bind to immobilized NECABs was *N*-copine, yet another neuronal multi-domain protein. Moreover, the localizations of all of these proteins exhibit little similarity. NECAB 1 is synthesized in a restricted set of neurons whereas Syt 1 and Mint 2 are expressed in all neurons in forebrain. Furthermore, NECAB 1 fills the entire cytosol whereas Syt 1 is exclusively synaptic (reviewed in Südhof and Rizo, 1996) and Mint 2 is enriched in the Golgi apparatus (unpublished observation). Although it is conceivable that *N*-copine is the physiological interactor for NECAB 1, it is also not colocalized with NECAB 1 (Nakayama et al., 1999), and the most likely explanation is that NECABs, Syt 1, and other binding proteins are simply 'sticky' proteins.

Clues to the possible function of NECABs come from its domain structure and its localization. In terms of domain structure, the fusion of an N-terminal EF-hand Ca^{2+}-binding domain to C-terminal sequences suggests that Ca^{2+}-binding to the EF-hand may regulate the C-terminal sequences. Although the data bank searches revealed that the C-terminal sequences of NECABs contain an identifiable domain which is evolutionarily old since it has up to now only been detected in bacteria, unfortunately this domain has no known function, and thus does not provide information about the biological role of NECABs. It is curious, however, that although NECABs contain an evolutionarily old domain, they are themselves not evolutionarily conserved, but appear to be an invention of the vertebrate lineage. Thus two ancient domains, EF-hands and DUF176 domains, were combined in NECABs in vertebrates to produce a novel protein. In terms of localization, the restricted expression of NECAB 1 in a subset of neurons suggests that it has a specialized, as opposed to a general, function in neurons. This conclusion again agrees with the lack of NECABs in invertebrates since any fundamental neuronal function should be operating in invertebrates as well. Future experiments will have to address these important issues.

Acknowledgements—We would like to thank C. Moomaw, S. Afendis, and Dr. C. Slaughter for support in the amino acid sequencing of NECABs, and F. Schmitz and M. Missler for advice. This study was supported by postdoctoral fellowships from the Muscular Dystrophy Association to S.S., and from the NIH to A.H.

Fig. 8. Domain structure of NECABs. (A) Diagram of the NECAB domain structure (NHR = NECAB homology region). (B) Alignment of the N-terminal sequences of NECAB 1, 2 and 3 with the sequences of EF-hand Ca^{2+}-binding domains. In the EF-hand, a Ca^{2+}-binding loop is flanked by two α-helices. Residues characteristic of EF-hand Ca^{2+}-binding sites are shown between the NECAB and EF-hand sequences; these include hydrophobic amino acids on the inner face of the two α-helices (identified by 'n'), and characteristically spaced residues in the Ca^{2+}-binding loop that coordinate the Ca^{2+} ion (marked by '*'). In addition, the Ca^{2+}-binding loop contains an obligatory central glycine residue ('G') followed by a variable residues and a hydrophobic amino acid (ø). Note that NECABs correspond precisely to the consensus sequence for EF-hand Ca^{2+}-binding sites. Shared residues are highlighted in white on a black background for identical amino acids, and in white on a gray background for similar amino acids (similarity groups: D, E; R, K; S, T; N, Q; Y, F; hydrophobic residues). (C) Alignment of the N-terminal sequences of NECAB 1, 2 and 3 with the sequences of the DUF176 domains from bacteria as identified in the NCBI conserved domain database. The C-terminal NECAB sequences (NECAB 1, 2 and 3) are compared with the DUF176 domain from bacterial DUF176 containing proteins identified by acronyms on the left. Shared residues are highlighted as described for B.

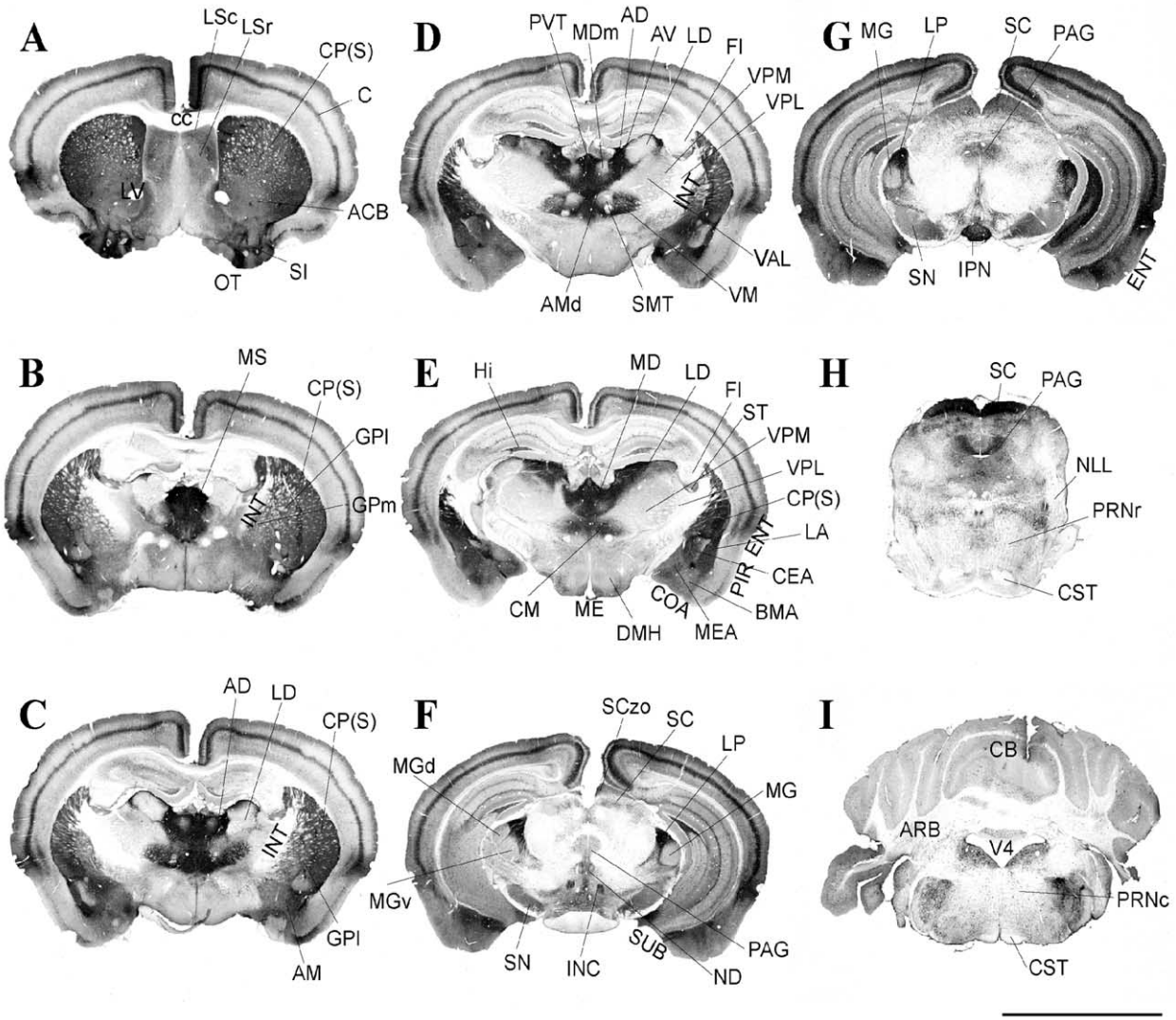

Fig. 10. Immunolocalization of NECAB 1 in mouse brain sections. Coronal sections at different levels were reacted with affinity-purified NECAB 1 antibodies, and stained with HRP-coupled secondary antibodies with metal enhancement. Note the restricted expression of NECAB 1 in subsets of neurons, e.g. layer 4 of the cerebral cortex, the entire striatum, and a subset of thalamic nuclei whereas many other neurons (e.g. most of the hippocampal and cortical pyramidal neurons and the entire cerebellar cortex) and white matter (e.g. the corpus callosum and the interior capsule) remain unlabeled. Abbreviations used: ACB, nucleus accumbens; AD, anterodorsal nucleus of the thalamus; AMD, antero-medial nucleus of the thalamus; ARB, arbor vitae (medulla cerebellum); AV, anteroventral nucleus of the thalamus; BMA, basomedial nucleus of the amygdala; C, cerebral cortex; CB, cerebellum; Cc, corpus callosum; CEA, central nucleus of the amygdala; CM, central medial nucleus of the thalamus; COA, cortical nucleus of the amygdala; CP (S), caudoputamen (striatum); CST, corticospinal tract (pyramidal tract); DMH, dorsomedial nucleus of the hypothalamus; ENT, entorhinal area; FI, fimbria hippocampi; GPM, globus pallidus, lateral segment; GPI, globus pallidus, medial segment; Hi, hippocampus; INC, interstitial nucleus of Cajal; IPN, interpeduncular nucleus; INT, internal capsule; LA, lateral nucleus of the amygdala; LD, lateral dorsal nucleus of the thalamus; LP, lateral posterior nucleus of the thalamus; LV, lateral ventricle; LSc, lateral septal nucleus, caudal part; LSr, lateral septal nucleus, rostral part; MD, mediodorsal nucleus of the thalamus; MDm, mediodorsal nucleus of the thalamus, medial part; ME, median eminence; MEA, medial nucleus of the amygdala; MG, medial geniculate complex of the thalamus; MGd, medial geniculate complex of the thalamus, dorsal part; MGv, medial geniculate complex of the thalamus, ventral part; MS, medial septal nucleus; ND, nucleus of Darkschewitsch; NLL, nucleus of the lateral leminiscus; OT, olfactory tubercle; PAG, periaqueductal gray; PIR, piriform cortex; PRNc pontine reticular nucleus, caudal part; PRNr, pontine reticular nucleus, rostral part; PVT, paraventricular nucleus of the thalamus; SC, superior colliculus; SC zo, colliculus superior, zonal layer; SI, substantia innominata; SMT, submedial nucleus of the thalamus; SN, substantia nigra; ST, stria terminalis; SUB, subiculum; V4, fourth ventricle; VAL, ventral anterior lateral complex of the thalamus; VM, ventral medial nucleus of the thalamus; VPL, ventral posterolateral nucleus of the thalamus; VPM, ventral posteromedial nucleus of the thalamus. Scale bar = 4 mm.

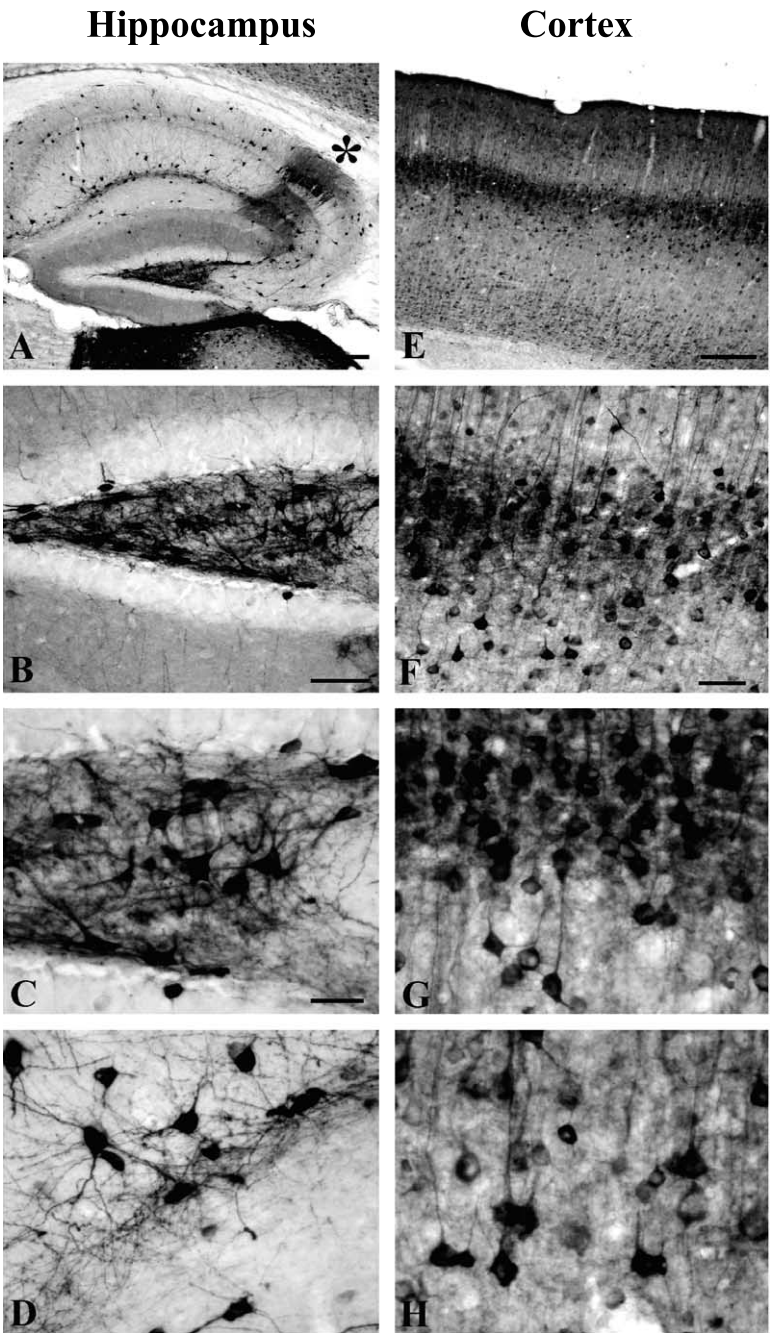

Fig. 11. Restricted expression of NECAB 1 in cerebral cortex and hippocampus. Panels show at increasing magnifications selected areas of the hippocampus and cortex stained for NECAB 1 as described in Fig. 10. Note that in the hippocampus (A–D), only interneurons contain NECAB 1 except for a wedge of pyramidal neurons in CA2 (asterisk in A). Interneurons in the hilus of the dentate gyrus are most strongly labeled (B). In these interneurons, the whole cell body and the dendrites appear to be filled with NECAB 1 (C and D). In the cerebral cortex, only layer 4 is strongly labeled although some immunoreactivity is also detectable in other layers, especially layer 2 (E). In layer 4, the labeling appears to be concentrated in projection neurons (F) which are uniformly stained except for the nucleus (G and H) similar to the hippocampal neurons. Scale bars = 0.3 mm (A); 0.2 mm (B, E); 20 μm (C, D, G, H); 0.1 mm (F).

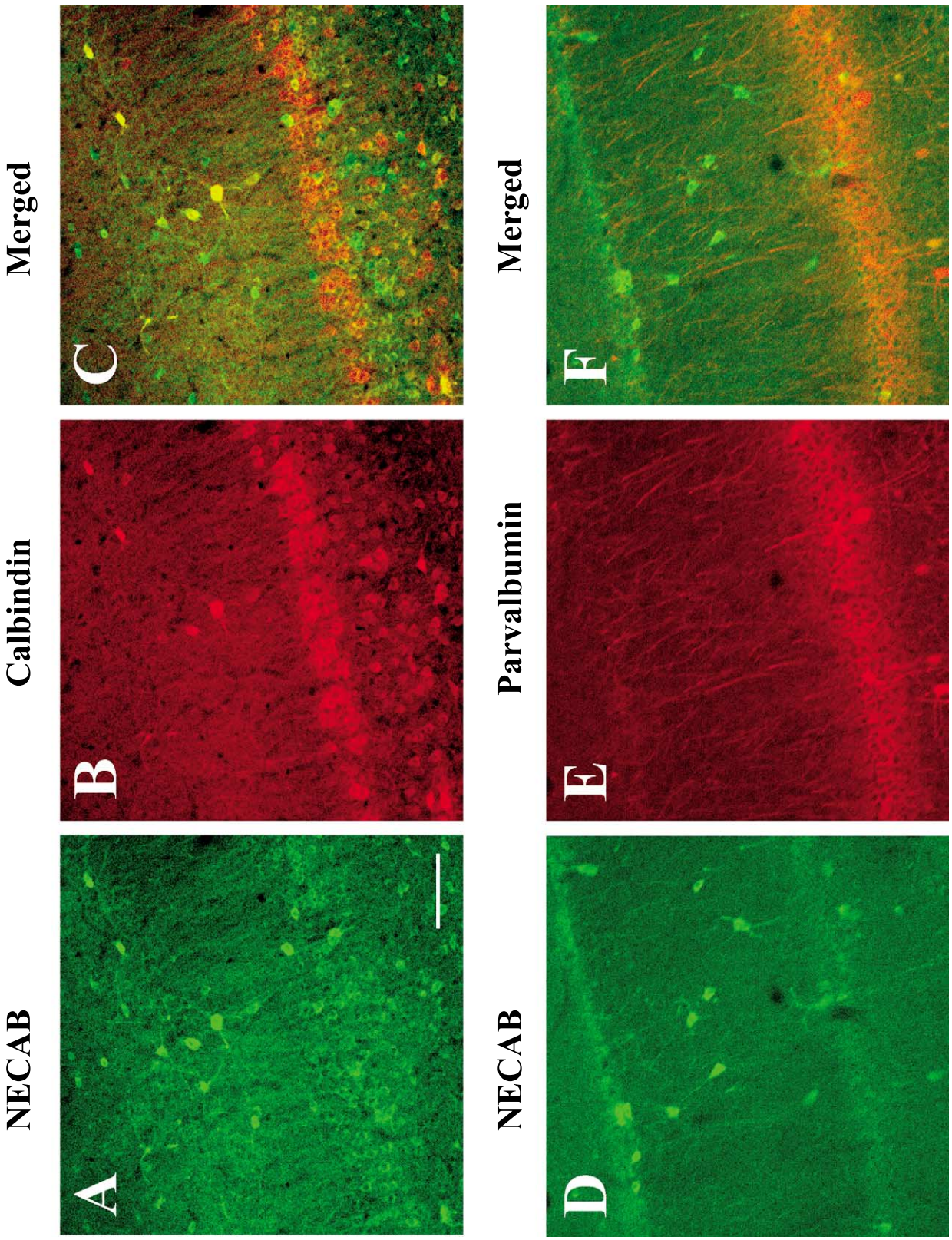

Fig. 12. Comparison of the distribution of NECAB 1 and two other EF-hand Ca^{2+}-binding proteins (calbindin and parvalbumin) in hippocampus using double immunofluorescence labeling. Cryostat sections were double-labeled for NECAB 1 and calbindin (A–F) or NECAB 1 and parvalbumin (G–L). Note that NECAB 1 has a wider distribution among interneurons than calbindin, although all calbindin-positive neurons contain also NECAB 1. Scale bar = 30 μm.

REFERENCES

Baimbridge, K.G., Celio, M.R., Rogers, J.H., 1992. Calcium-binding proteins in the nervous system. Trends Neurosci. 15, 303–308.

Braunewell, K.H., Gundelfinger, E.D., 1999. Intracellular neuronal calcium sensor proteins: a family of EF-hand calcium-binding proteins in search of a function. Cell Tissue Res. 295, 1–12.

Caillard, O., Moreno, H., Schwaller, B., Llano, I., Celio, M.R., Marty, A., 2000. Role of the calcium-binding protein parvalbumin in short-term synaptic plasticity. Proc. Natl. Acad. Sci. USA 97, 13372–13377.

Daly, C., Ziff, E.B., 1997. Post-transcriptional regulation of synaptic vesicle protein expression and the developmental control of synaptic vesicle formation. J. Neurosci. 17, 2365–2375.

Davletov, B.A., Südhof, T.C., 1993. A single C_2-domain from synaptotagmin I is sufficient for high affinity Ca^{2+}/phospholipid-binding. J. Biol. Chem. 268, 26386–26390.

Donato, R., 2001. S100: a multigenic family of calcium-modulated proteins of the EF-hand type with intracellular and extracellular functional roles. Int. J. Biochem. Cell Biol. 33, 637–668.

Geppert, M., Goda, Y., Hammer, R.E., Li, C., Rosahl, T.W., Stevens, C.F., Südhof, T.C., 1994. Synaptotagmin I: a major Ca^{2+}-sensor for transmitter release at a central synapse. Cell 79, 717–727.

Guan, K.L., Dixon, J.E., 1991. Eukaryotic proteins expressed in *Escherichia coli*: an improved thrombin cleavage and purification procedure of fusion proteins with glutathione *S*-transferase. Anal. Biochem. 192, 262–267.

Gulyas, A.I., Megias, M., Emri, Z., Freund, T.F., 1999. Total number and ratio of excitatory and inhibitory synapses converging onto single interneurons of different types in the CA1 area of the rat hippocampus. J. Neurosci. 19, 10082–10097.

Hof, P.R., Glezer, I.I., Conde, F., Flagg, R.A., Rubin, M.B., Nimchinsky, E.A., Vogt Weisenhorn, D.M., 1999. Cellular distribution of the calcium-binding proteins parvalbumin, calbindin, and calretinin in the neocortex of mammals: phylogenetic and developmental patterns. J. Chem. Neuroanat. 16, 77–116.

Kawasaki, H., Nakayama, S., Kretsinger, R.H., 1998. Classification and evolution of EF-hand proteins. Biometals 11, 277–295.

Kee, Y., Scheller, R.H., 1996. Localization of synaptotagmin-binding domains on syntaxin. J. Neurosci. 16, 1975–1981.

Laemmli, U.K., 1970. Cleavage of structural proteins during the assembly of the head of bacteriophage T4. Nature 227, 680–685.

Lee, D.S., Tomita, S., Kirino, Y., Suzuki, T., 2000. Regulation of X11L-dependent amyloid precursor protein metabolism by XB51, a novel X11L-binding protein. J. Biol. Chem. 275, 23134–23138.

Lewit-Bentley, A., Rety, S., 2000. EF-hand calcium-binding proteins. Curr. Opin. Struct. Biol. 10, 637–643.

Li, C., Ullrich, B., Zhang, J.Z., Anderson, R.G.W., Brose, N., Südhof, T.C., 1995. Ca^{2+}-dependent and Ca^{2+}-independent activities of neural and nonneural synaptotagmins. Nature 375, 594–599.

Maruyama, K., Mikcawa, T., Egashi, S., 1984. Detection of calcium binding proteins by ^{45}Ca autoradiography on nitrocellulose membrane after sodium dodecyl sulfate gel electrophoresis. J. Biochem. (Tokyo) 95, 511–519.

Nakayama, T., Yaoi, T., Kuwajima, G., 1999. Localization and subcellular distribution of *N*-copine in mouse brain. J. Neurochem. 72, 373–379.

Nakayama, T., Yaoi, T., Yasui, M., Kuwajima, G., 1998. *N*-copine: a novel two C2-domain-containing protein with neuronal activity-regulated expression. FEBS Lett. 428, 80–84.

Nelson, M.R., Chazin, W.J., 1998. Structures of EF-hand Ca^{2+}-binding proteins: diversity in the organization, packing and response to Ca^{2+} binding. Biometals 11, 297–318.

Nguyen, T., Südhof, T.C., 1997. Binding properties of neuroligin 2 and neurexin 1β reveal function as heterophilic cell adhesion molecules. J. Biol. Chem. 272, 26032–26039.

Perin, M.S., Fried, V.A., Mignery, G.A., Jahn, R., Südhof, T.C., 1990. Phospholipid binding by a synaptic vesicle protein homologous to ther regulatory region of protein kinase C. Nature 345, 260–261.

Rizo, J., Südhof, T.C., 1998. C_2-domains, structure of a universal Ca^{2+}-binding domain. J. Biol. Chem. 273, 15879–15882.

Sambrook, J., Fritsch, E.F., Maniatis, T., 1989. Molecular Cloning: a Laboratory Manual, 2nd edn. Cold Spring Harbor Laboratory, Cold Spring Harbor, NY.

Shao, X., Li, C., Fernandez, I., Zhang, X., Südhof, T.C., Rizo, J., 1997. Synaptotagmin–syntaxin interaction: the C_2-domain as a Ca^{2+}-dependent electrostatic switch. Neuron 18, 133–142.

Sorimachi, H., Suzuki, K., 2001. The structure of calpain. J. Biochem. (Tokyo) 129, 653–664.

Südhof, T.C., Rizo, J., 1996. Synaptotagmins: C_2-domain proteins that regulate membrane traffic. Neuron 17, 379–388.

Sugita, S., Ichtchenko, K., Khvotchev, M., Südhof, T.C., 1998. α-Latrotoxin receptor CIRL/latrophilin 1 (CL1) defines an unusual family of ubiquitous G-protein-linked receptors. J. Biol. Chem. 273, 32715–32724.

Sugita, S., Südhof, T.C., 2000. Specificity of Ca^{2+}-dependent protein interactions mediated by the C_2A domains of synaptotagmins. Biochemistry 39, 2940–2949.

Towbin, H., Staehelin, T., Gordon, J., 1979. Electrophoretic transfer of proteins from polyacrylamide gels to nitrocellulose sheets: procedure and some applications. Proc. Natl. Acad. Sci. USA 76, 4350–4354.

Ubach, J., Zhang, X., Shao, X., Südhof, T.C., Rizo, J., 1998. Ca^{2+} binding to synaptotagmin: how many Ca^{2+} ions bind to the tip of a C_2-domain. EMBO J. 17, 3921–3930.

Vecellio, M., Schwaller, B., Meyer, M., Hunziker, W., Celio, M.R., 2000. Alterations in Purkinje cell spines of calbindin D-28 k and parvalbumin knock-out mice. Eur. J. Neurosci. 12, 945–954.

Wasinger, V.C., Humphery-Smith, I., 1998. Small genes/gene-products in *Escherichia coli* K-12. FEMS Microbiol. Lett. 169, 375–382.

Zhang, X., Rizo, J., Südhof, T.C., 1998. Mechanism of phospholipid binding by the C_2A-domain of synaptotagmin I. Biochemistry 37, 12395–12403.

(*Accepted* 31 *January* 2002)